Bio-Medical Materials and Engineering 26 (2015) S1201–S1211
DOI 10.3233/BME-151417
IOS Press

Anticorrelated networks in resting-state fMRI-BOLD data

Yadong Liu[a,b], Liangming Huang[a], Ming Li[a], Zongtan Zhou[a] and Dewen Hu[a,*]
[a]*College of Mechatronics and Automation, National University of Defense Technology, Changsha, Hunan 410073, P.R. China*
[b]*State key laboratory of high performance computing, National University of Defense Technology, Changsha, Hunan 410073, P.R. China*

Abstract. In this work, abundant anticorrelated networks were successfully detected in rest-stating fMRI-BOLD data from 20 subjects. Spatial independent component analysis (sICA) method was applied at both individual and group levels. At the individual level, for each subject, 30 independent components (IC) were estimated, and each IC was transformed using Z-score mapping. The voxels with >5 and < -5 Z-score were denoted as positive signals (PS) and negative signals (NS) respectively. The correlation coefficients between the mean time series of the PS and NS voxels were computed; if the calculated coefficients were <-0.3, the PS and NS voxels were considered to form an anticorrelated PS-NS network. It was found that 36.5% of the ICs contained an anticorrelated PS-NS network. The spatiotemporal patterns of most PS-NS networks varied from subject to subject, but three networks displaying spatial patterns were comparably consistent among different subjects. For group-level analysis, no anticorrelated PS-NS networks were detected. Our results suggest that future investigations adopt a broader approach for negative BOLD signal characterization. Combined consideration of PS and NS systems help to better elucidate hemodynamic and neuronal brain behavior and further develop understanding of neural mechanisms of brain information processing.

Keywords: Negative BOLD signal, resting-state network, anticorrelated network, low frequency fluctuation

1. Introduction

In fMRI, to date, most efforts have been directed in the selection of stimuli-induced BOLD responses. Generally, these efforts have disregarded resting-state signal components, which may discard potentially useful information for understanding brain behavior. However, recently there has been growing interest in resting-state fMRI. Some studies have revealed that neurons are not actually silent during rest [1], but still influence each other through excitatory and inhibitory synaptic connections and tend to present correlated dynamics. Thus, it is feasible to explore functional connected networks by using synchronous intrinsic BOLD signals in resting-state fMRI [2].

Functional connectivity is defined as the synchronization of neurophysiological events among anatomically separated areas. This definition was first introduced for PET and later applied for fMRI [3]. Biswal and his colleagues [4] were the first to report that during rest, the primary motor regions in

* Address for correspondence: Dewen Hu, College of Mechatronics and Automation, National University of Defense Technology, Changsha, Hunan 410073, PR China. Tel.: +86073184574992; E-mail: dwhu@nudt.edu.cn.

the left and right hemispheric present synchronous BOLD signals, which can be used to recover motor networks. Further studies [2] demonstrated similar resting-state networks in primary visual regions, auditory regions, and some high order cognitive regions etc. These networks are often referred as resting-state networks and can be robustly detected using different groups of subjects and diverse methods. The fMRI signals sent between these resting-state networks present high levels of co-activation and have been used as major measurement for the characterization of the functional network in resting-state.[2, 5, 6, 7] As of now, there have been eight reported functionally connected sub-networks in resting-state: primary sensorimotor network, primary visual and extra-striate visual network, two lateralized parietal-frontal networks consisting of superior parietal and superior frontal regions, default-mode network, the network consisting of bilateral temporal/insular and anterior cingulate cortex regions, and medial temporal lobe network [2]. Several recent studies supply strong physiological support for detecting the above networks in resting-state fMRI. Studies combining resting-state fMRI with structural diffusion tensor imaging measurements suggested a direct correlation between functional and structural connectivity in the human brain [8]. A combined human EEG and fMRI investigation suggested a direct association between neural activity and resting-state fMRI fluctuation signals [9] and simultaneous invasive electrophysiology and BOLD recording in anesthetized monkeys also established correlation between neuronal activity and fluctuation BOLD signals [10].

In addition to widely reported correlated resting-state networks, anticorrelated networks were also revealed in a few studies. Fox reported that, when subjects were in rest with their eyes fixed on a crosshair, an anticorrelated network could be recovered, consisting of regions involving PCC, MPF, LP (correlated) and IPS, FEF, MT, SMA, and insula (anticorrelated). Other studies [11] reported a similar resting-state anticorrelated network consisting of PCC, MPFC, R. & L. angular gyrus (correlated) and R. & L. insula, R. & L. DLPFC, R. & L. SMG (anticorrelated). Currently, the investigation on the origin of anticorrelated resting-state networks is far from closure. An artifact origin has also been proposed as the data suggests anti-correlation may be introduced by global signal regression, and therefore, should be interpreted very carefully. Some other studies [12] suggest a neural source. It was suggested that an anticorrelated network is induced by the synchronous activation of excitatory and inhibitory neurons. It should be noted that the above works, supporting or arguing against a meaningful origin of anticorrelated networks, are indeed carried in the context of the default-mode network. The possibility of more abundant anticorrelated networks is not excluded.

In this work, a sICA-based procedure was proposed to successfully explore abundant anticorrelated networks in closed-eye resting-state fMRI. Of importance is that we found three spatially consistent anticorrelated networks across subjects. We thought these networks reflect a cooperation or opposition mechanism in a global scale of the brain. Compared with investigating correlated networks alone, a combined consideration of anticorrelated PS and NS networks may widen a horizon of brain functional connectivity.

2. Materials and methods

2.1. Experiment design and data acquisition

Twenty neurologically healthy volunteers (10 males and 10 females; mean age, 29 years; age range, 18-26 years) without a history of neurological and psychiatric disorders were recruited. They received instructions to close their eyes, maintain a relaxed state, remain awake and perform no specific

cognitive exercise. All subjects verified that a conscious state was maintained throughout the procedure. MRI scans were performed with a 1.5T GE Signa System (GE Signa, Milwaukee, Wisconsin, USA). To reduce head movements, subjects' heads were fixed using foam pads with a standard birdcage head coil. The fMRI images were collected using a gradient-echo EPI sequence (TR=2000 ms, TE=40 ms, FOV=24 cm, FA= 90°, matrix=64×64, slice thickness=5 mm, gap=1 mm, slices=20). Each functional resting-state session lasted eight minutes, and 240 volumes were obtained.

2.2. Data analysis

No global regression was applied in this study as its utilization has been demonstrated to introduce anti-correlation; to eliminate this possibility, global regression was not incorporated [13].

The data were analyzed at both the individual level and group level. The analysis procedure consisted of three steps. In step 1, for each subject, the first 5 volumes of the scanned data were discarded for magnetic saturation effects by applying the statistical parametric mapping software package. The remaining 235 volumes were corrected by registering and reslicing for head motion. All subjects in this study had less than 1 mm translation in x, y, or z-axis and 1° of rotation in each axis. After the head motion effect was removed, the volumes were normalized to the standard EPI template in the Montreal Neurological Institute (MNI) space.

We avoided any spatial smoothing to preserve spatial resolution [14, 15]. In step 2, principle component analysis (PCA) was employed to reduce the dimensionality of original data to 30 guaranteeing over 99% power of original data was hold. sICA algorithm with tanh(·) as the nonlinearity was used to apply ICA processing at both individual and group level [16]. ICs were estimated in a parallel manner. In step 3, each spatial IC was transformed into *Z*-score mapping. The voxels with >5 and < -5 *Z*-score were selected out respectively with whose mean time series being generated. The correlation coefficients between PS and NS mean time series for all ICs were computed for further analysis.

The whole procedure is outlined in the flow chart shown in Figure 1. For sake of discussion, we defined the mean time series for >5 and <-5 *Z*-score voxels as PS and NS respectively. When the correlation coefficient between PS and NS was below -0.3, we called the associated networks as PS-NS network.

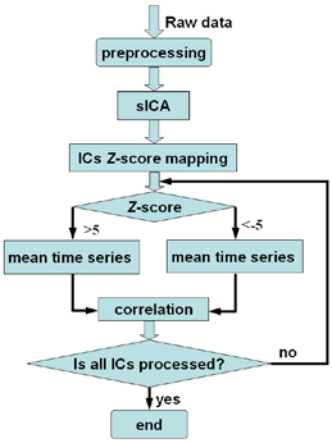

Fig. 1. Flow chart for data analysis procedure.

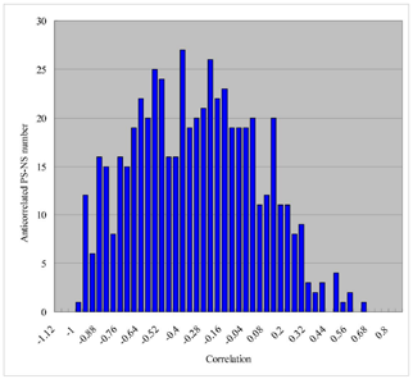

Fig. 2. The histogram of correlation coefficients between PS and NS.

3. Results

For individual-level analysis, the above procedure was applied to each subject's data separately. A great deal of PS-NS networks were detected, the majority of which were subject-specific, while three PS-NS networks were found to be comparatively consistent across subjects. For group-level analysis, there were eight reported correlated resting-state networks that were successfully extracted, however, no PS-NS networks were detected.

3.1. Analysis of individual level

For each subject, data were analyzed independently, and 30 ICs were estimated. For the 600 collected ICs, 36.5% (219) presented <-0.3 correlation coefficients resulting in 219 PS-NS networks; the mean correlation coefficient of the 219 PS-NS networks was -0.6018. A histogram of correlation coefficients is displayed in Figure 2.

While a majority of the 219 PS-NS networks were subject-specific, the spatial as well as temporal patterns of major PS-NS networks varied across subjects, three PS-NS networks were found to be consistent throughout the group.

An example for each consistent PS-NS network are shown in Figures 3-5 and the detailed regions contained in each network are given in Tables 1-3, respectively. Two examples of inconsistent networks are presented in Figure 6. In all figures, the PS and NS voxels are represented in red and blue respectively. The voxels' colors were mapped by their *Z*-score values.

An example of the first consistent PS-NS network is shown in Figure 3. Similar networks, as listed in Table 2, were detected in four subjects in total. In these networks, the PS sub-network is comprised of the primary motor, SMA and insular-temporal/ACC regions. The primary motor and insular-temporal/ACC regions were regarded as two discrete networks in prior studies [2]. The NS sub-network was found to consist of small isolated regions in frontal, PPC and primary visual areas. It can be seen in Table 2 that, if present, the regions of PS sub-networks were more consistent than those of NS sub-networks. Three PS regions, i.e. primary motor, SMA and insular-temporal/ACC, were present in all four subjects while only one NS region, the frontal region, was detected in all four subjects. The PPC and primary visual regions, which are also NS regions, were present in two subjects and one subject respectively. For convenience of discussion, this pattern is referred to as PS-NS network 1.

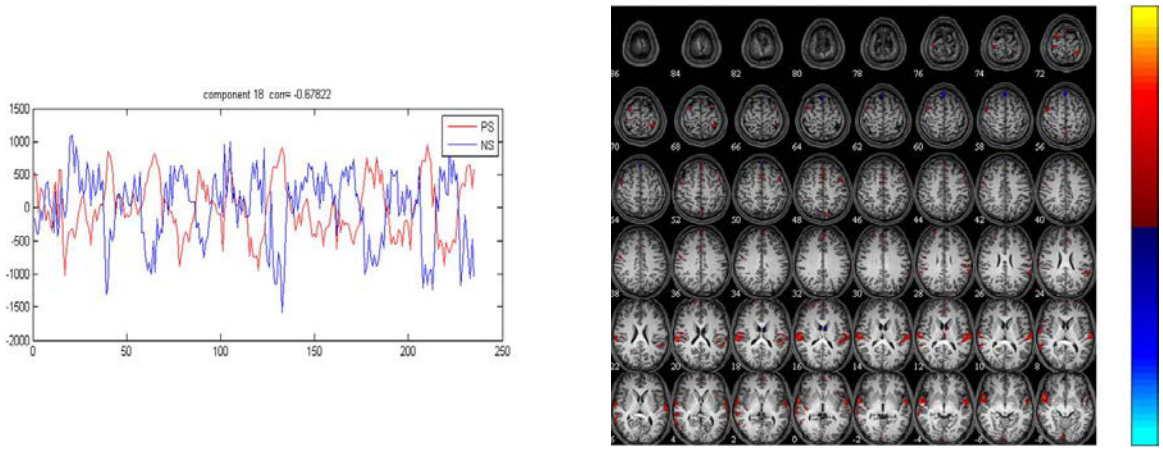

Fig. 3. An example of PS-NS network 1. Similar networks were detected in four subjects.

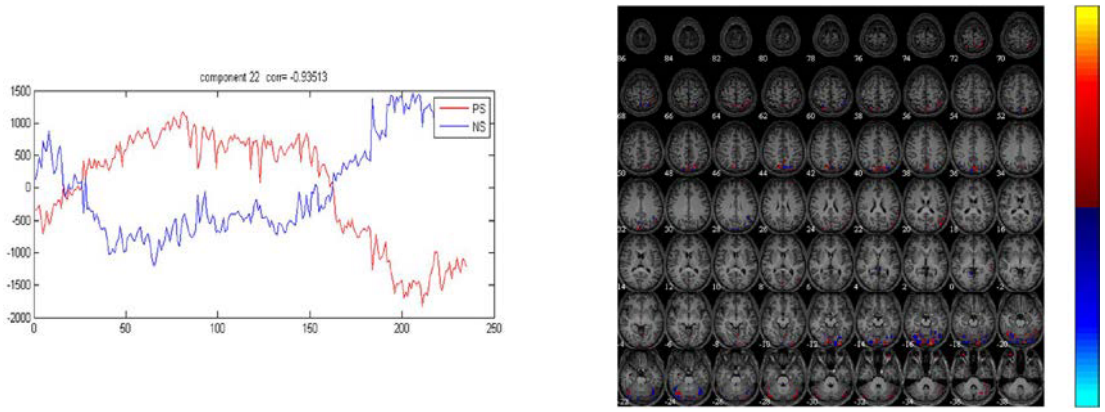

Fig. 4. An example of PS-NS network 2. The network consists of regions in primary visual, extra-striate visual, frontal and cerebellum. Similar networks were detected in eight subjects.

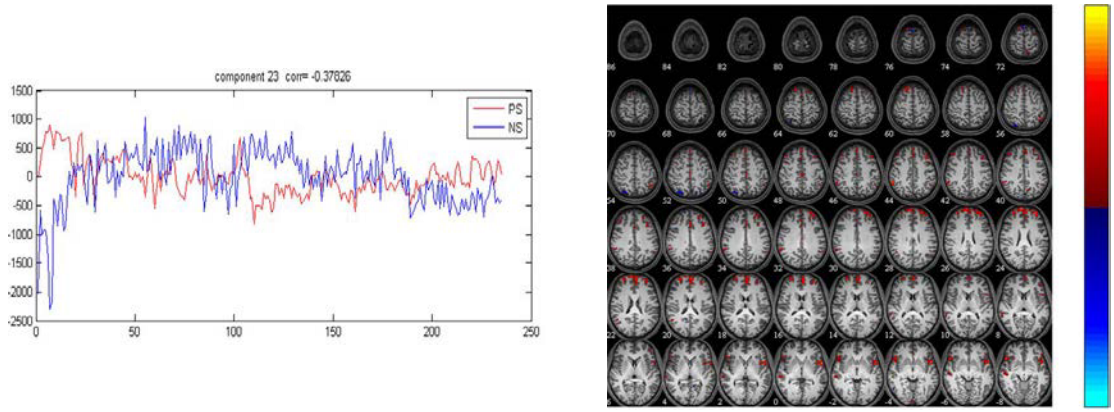

Fig. 5. An example of PS-NS network 3. The PS sub-network is the popularly reported default-mode network. Similar networks were detected in seven subjects.

Table 1

The numbers of PS-NS networks for twenty subjects

	1	2	3	4	5	6	7	8	9	10	11	12	13	14	15	16	17	18	19	20
network number	6	16	17	8	5	13	12	15	10	10	4	9	9	10	13	11	8	18	14	11

Note: Ten for females and the others for males.

Table 2

Detailed regions of PS-NS network 1 in twenty subjects

subject	1	8	13	19
Primary motor	P	P	P	P
SMA	P	P	P	P
Insular-temporal/ACC	P	P	P	P
Frontal region	N	N	N	N
PPC	N	*	*	N
Primary visual	*	N	*	*

Note: 'P' denotes the region presents PS, 'N' denotes the regions present NS, and '*' denotes neither PS nor NS presents.

Table 3

Detailed regions of PS-NS network 2 in twenty subjects

subject	1	3	7	9	13	14	16	20
Frontal	*	P	*	*	*	*	*	P/N
PPC	*	P	P	P/N	*	P/N	*	*
Primary visual	N	P	P/N	P/N	P/N	P/N	P/N	P/N
Extra-striate visual	P/N	N	P/N	P/N	P/N	P/N	P/N	P/N
Cerebellum	P/N	P/N	P/N	P/N	P/N	P/N	P/N	P/N

Note: 'P' denotes the region presents PS, 'N' denotes the regions present NS, and '*' denotes neither PS nor NS presents.

Table 4

Detailed regions of PS-NS network 3 in twenty subjects

subject	1	9	10	15	17	18	19
Default-mode	P	P	P	P	P	P	P
Frontal	N	*	*	*	*	N	N
PPC	*	N	N	N	N	*	N
Insular-temporal/ACC	*	N	N	N	N	N	N

Note: 'P' denotes the region presents PS, 'N' denotes the regions present NS, and '*' denotes neither PS nor NS presents.

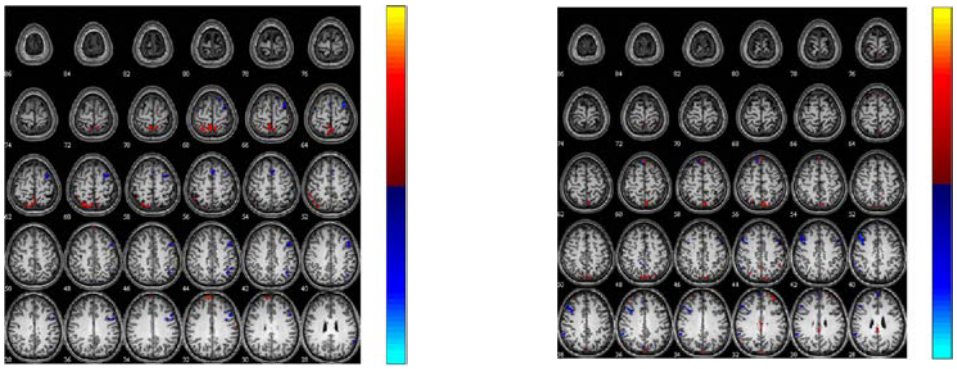

a b

Fig. 6. a) A PS-NS network locating in right parietal-frontal, frontal and PPC areas. It was detected in only one subject. b) A PS-NS network locating in left parietal-frontal, frontal and PPC areas. It was detected in only one subject.

The second consistent PS-NS network is given in Figure 4 and was shown to consist of structures from the frontal, PPC, primary visual, cerebellum and extra-striate visual regions. In these regions, PS and NS regions are interlaced with each other if they are presented. Similar patterns were detected in eight subjects, and are listed in Table 3 and are referred to as PS-NS network 2.

Shown in Figure 5, the third consistent PS-NS network consisted of a popularly reported default-mode network and some foci in frontal and PPC regions. The PS sub-network is the default-mode network comprised of precuneus, medial frontal, inferior parietal cortical regions and medial temporal lobe. The NS sub-network is made up of the frontal and PPC regions. Similar patterns were detected in seven subjects and detailed regions from the subjects are listed in Table 4. This pattern is referred to as PS-NS network 3.

The above three PS-NS networks were comparatively robust patterns embedded in the data from the

twenty subjects. As most PS-NS networks detected in our work were inconsistent across subjects for both spatial and temporal dimensionality, it was impossible to fully illuminate the properties of the described networks. Two inconsistent PS-NS networks from different subjects are given in Figure 6. The left parietal-frontal and right parietal-frontal resting-state networks are presented as NS sub-networks. The PS sub-network consisted of the PPC and frontal regions.

3.2. Analysis of group level

For group-level analysis, group-sICA was applied to the aggregate data of the twenty subjects. The general reported eight resting-state networks described previously were all successfully extracted, while no consistent PS-NS network was detected. The following reasons may account for the lack of detection: 1) PS-NS networks tend to be subject-specific. Although the three consistent PS-NS networks were detected in several subjects when sICA was applied to subjects individually, they were not explicit enough to espy in the group-level analysis. This etiological explanation may account for the lack group-level discernment of network 1 which was only detected in 4 subjects. Furthermore, the NS regions among networks 1, 2 and 3 were present in less subjects compared with the PS regions, as shown in Tables 1-3. This made consistent detection more difficult for PS-NS networks in group analysis. 2) The lack of spatiotemporal distinction of PS and NS regions in certain brain areas coupled with the variation in location of PS and NS voxels from subject to subject, resulted in inconsistent PS-NS networks in the group-ICA analysis. This may account for the resultant grouping in network 2.

4. Discussion

The functional role of PS-NS networks in resting-states is in dire need of further investigation. The opposite signs of PS and NS seem to indicate some cooperative or antagonistic mechanism of information processing in the brain across different spatiotemporal scales. Fox et al. [6] suggested that "while correlations may serve as an integrative role in combining neuronal activity subserving similar goals or representations, anticorrelations may serve as a differentiating role segregating neuronal processes subserving opposite goals or competing representations". Hampson et al. [13] also posited "anticorrelation can also serve as an integrative role, allowing regions to share and process information together".

4.1. The physiological origin of anticorrelated PS-NS networks

Discovering the anticorrelated PS-NS networks is one task, while understanding its function and its role in behavior and cognition is another entirely. PS-NS networks may have either neuronal or vascular sources. A neuronal origin is reflection of some underlying information processing of neural networks which attracts most neuroscientists and information scientists, hence it deserves a more comprehensive investigation; A vascular origin is of less importance, but still deserves study in hemodynamic.

As identification and understanding of the nexus of PS-NS networks requires comprehensive investigation, this study seeks only to discuss the possible causal mechanisms and the associated ramifications.

It is well known that BOLD signals themselves do not directly measure the neuronal activity. This a result of the numerous components of neuronal activity, including intrinsic fluctuations, EPSPs, IPSPs,

action potential generation and propagation along the axon, and release, binding, reuptake, and reprocessing of the released neurotransmitter. The BOLD signal may be induced by one component alone or by the aggregate effects of several components; The PS-NS network may adhere to a similar mechanism. The origin of PS-NS network may be a result of the coupling increase and decrease of local activity (EPSPs, IPSPs, action potential generation and propagation along the axon), the blood supply or the anticorrelated changes associated with neurotransmitter of the PS and NS areas.

The source of coupling increase and decrease of local neuronal activity may hint that: (1) PS-NS networks may be the reflection of underlying information processing mechanisms in a resting-state. PS and NS regions carry out different but correlated cognition tasks, for example the maintenance of necessary function of the brain in a resting-state or the preparation of the alarming and attending system for external and internal stimuli. This may be similar to so called default-mode networks, etc. (2) PS-NS networks may be the reflection of cooperative or antagonistic behavior that excitatory and inhibitory neurons exploit for necessary function. Both empirical and theoretical studies suggest that excitatory and inhibitory neurons are likely to be balanced, so that it is unreasonable that one would observe increase in one without an increase in the other [11]. The synchronous activation of excitatory and inhibitory neurons can result in corresponding synchronous action upon target neurons, assembling PS and NS networks respectively. (3) The PS-NS network may be the result of a pair of anti-phase coupling LFPs. The primary component of the BOLD signal is LFP, which measures slow waveforms such as synaptic potentials, afterpotentials of somato-dendritic spikes, and voltage-gated membrane fluctuations. Hence, LFPs contain rich information including input signals and the local intracortical processing actions mediated by the sub-threshold signals of interneurons. In general, neurons fire and transfer spikes to subsequent neurons when their EPSP/IPSP are beyond some firing threshold. This threshold is not at the zero firing level but the time-varied value in accordance to local LFP. A time-varied LFP results in a time-varied firing threshold, which means that low LFP results in low firing threshold and neurons are apt to be excited, while a high LFP results in high firing threshold and neurons are susceptible to inhibition. A firing threshold oscillating with the time-varied LFP sequentially generates periodic activation of cortical regions. Hence, two regions with anti-phase coupling LFPs exhibit anti-phase coupling BOLD signals. If this explanation accounts for the genesis of this phenomenon, the resulting two regions would display an anti-phase LFP. To validate this hypothesis, direct measuring on LFP would be required.

The source of emergence of coupling increase and decrease of blood supply may indicate a dynamic blood purvey mechanism in resting-state [19]. Blood is distributed to each region in a fluctuating fashion. When a region is supplied more blood than necessary, the supply will decrease, and more blood will flow to deficient regions. Because excess blood is received, the blood-lacking regions become blood-rich while the inverse occurs in the former blood-rich regions, a reverse blood flow occurs. This process will repeat continuously resulting in coupling fluctuation of PS and NS networks at some balanced levels. It comes into question that, for most fluctuating PS-NS networks, the PS and NS regions are separated spatially in a manner that they cannot be supported by one vascular structure. This begs an explanation as to the lack of efficiency in spatial architecture and why the blood supply is needed to be regulated on such a large scale. Moreover, for only a few consistent spatial PS-NS networks were detected in our observation, blood supply regulation between PS and NS regions were subject-varied and time-varied in most situations. For clear validation of this blood supply causal mechanism, direct blood-measuring tools, such as a laser Doppler system, are required in further studies.

4.2. Fluctuating PS-NS networks

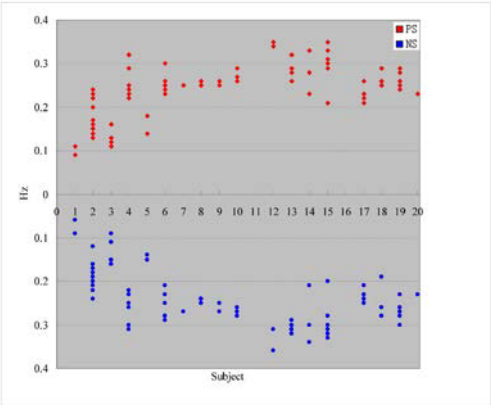

Fig. 7. Frequencies of fluctuations of PS and NS for twenty subjects.

Among all 219 PS-NS networks detected in this work, 29.7% (65) present were anticorrelated fluctuations. The frequencies of fluctuation varied from 0.05 to 0.36 Hz and the details are shown in Figure 7. A pair of anti-phase fluctuations may be a reflection of some kind of dynamic counterpoise among several antagonistic or cooperative of physiological mechanisms, as described in subsection 4.1.

In previous studies, fluctuations in resting-state are classified into three ranges: low-frequency (0~0.1 Hz), respiratory-frequency (0.1~0.5 Hz), and cardiac-frequency range (0.6~1.2 Hz) [5, 17, 18]. It must be noted that this is rough taxonomy. Among these three ranges, to date, low frequency fluctuation (LFF) signals (≈0.01-0.1 Hz) are of particular importance and have garnered substantial attention. LFF has been widely used in the exploration of functional networks [4], while only synchronous fluctuation, namely PS or NS alone, has been exploited in the recovery of functional networks. Generally, abundant PS-NS pairs are ignored in most studies.

It can be seen in Figure 7 that primary fluctuation in this study falls into the category of respiratory frequency. Additionally, it was observed that most PS and NS regions that presented fluctuations were located around the thalamencephalon and were embedded within each other. Hence, these PS-NS networks are more likely to be respiratory-associated which make them of less importance. It has already been reported that one can use the mean time series of an ROI in the thalamencephalon as a representation of respiratory signals. These representations can be incorporated into a design matrix in SPM to model the respiratory fluctuations. Our results showed that for most subjects, there were several pairs of respiratory-associated PS-NS fluctuations distributed in a comparable wide frequency range (Figure 7) with different pairs located at distinct regions. As a result, the utilization of the mean time series of randomly selected ROI to model the respiratory fluctuation may produce unsatisfactory consequences.

4.3. PS-NS default-mode network

Until recently, it was reported that default-mode networks could be detected under conditions of closed-eye rest in visual processing and attention-demanding cognitive tasks etc [20].

The PS-NS network associated with 'default-mode' network detected in this work was in the form a rest experiment where the network is evoked by intrinsic, internal stimuli. It is important to note that besides the well-known default-mode network, an anticorrelated network was detected in a low relative ratio. For the 20 rest data sets, ~80% sets presented the default-mode network, but only ~30% sets displayed the corresponding anticorrelated networks. If these anticorrelated networks do have a

neuronal origin, they have a potential functional significance, necessitating further characterization of the anticorrelated system for the comprehensive understanding of default-mode network.

5. Conclusions

In this study, it was found that there were anticorrelated PS-NS pairs in resting-state fMRI-BOLD data. To date, most studies have only investigated the task-related NS while neglecting the inactive components ones. This work suggests a broader approach should be constructed for NS investigation. Furthermore, our results suggest that, the combined investigation of PS and NS may improve our understanding of brain–behavior relationships. The spontaneously active PS-NS networks may raise intriguing questions regarding the ubiquitous hemodynamic and neuronal fluctuations and their as yet indeterminate functions. Cumulative incorporation of these systemic approaches may advance knowledge of neural mechanisms of information processing of the brain

Acknowledgments

This work is supported by Open Fund from HPCL (201403-03), and Natural Science Foundation of China (61473305).

References

[1] P. Martijn, H. Van den, E. Hilleke and P. Hulshoff, Exploring the brain network: A review on resting-state fMRI functional connectivity, European Neuropsychopharmacology **20** (2010), 519-534.
[2] M.P. Van Den Heuvel, R.C. Mandl and H.E. Hulshoff Pol, Normalized group clustering of resting-state fMRI data, PLoS One **3** (2008), e2001.
[3] K.J. Friston, P. Jezzard and R. Turner, Analysis of functional MRI time series, Human Brain Mapping **1**(1994), 153-171.
[4] B.B. Biswal, J. Van Kylen and J.S. Hyde, Simultaneous assessment of flow and BOLD signals in resting-state functional connectivity maps, NMR in Biomedicine **10(4-5)** (1997), 165-170.
[5] D. Cordes, V. Haughton, J.D. Carew, K. Arfanakis and K. Maravilla, Hierarchical clustering to measure connectivity in fMRI resting-state data, Magnetic Resonance Imaging **20(4)** (2002), 305-317.
[6] M.D. Fox and M.E. Raichle, Spontaneous fluctuations in brain activity observed with functional magnetic resonance imaging, Nature Reviews Neuroscience **8(9)** (2007), 700-711.
[7] C.F. Beckmann, M. DeLuca, J.T. Devlin and S.M. Smith, Investigations into resting-state connectivity using independent component analysis, Philosophical Transactions of the Royal Society of London, Series B **360(1457)** (2005), 1001-1013.
[8] P. Hagmann, L. Cammoun, X. Gigandet, R. Meuli, C.J. Honey, V.J. Wedeen and O. Sporns, Mapping structural core of human cerebral cortex, PLoS Biology **6(7)** (2008), e159.
[9] D.A. Leopold, Y. Murayama and N.K. Logothetis, Very slow activity fluctuations in monkey visual cortex: implications for functional brain imaging, Cereb Cortex **13** (2003), 422-433.
[10] A. Shmuel and D.A. Leopold, Neuronal correlates of spontaneous fluctuations in fMRI signals in monkey visual cortex: implications for functional connectivity at rest, Human Brain Mapping **29(7)** (2008), 751-761.
[11] X.Y. Long, X.N. Zuo, V. Kiviniemi, Y.H. Yang, Q.H. Zou, C.Z. Zhu, T.Z. Jiang, H. Yang, Q.Y. Gong, L. Wang, K.C. Li, S. Xie and Y.F. Zang, Default mode network as revealed with multiple methods for resting-state functional MRI analysis, Journal of Neuroscience Methods **171** (2008), 349-355.
[12] J.A. Owen and B. Simon, How well do we understand the neural origins of fMRI BOLD signals, Trends in Neurosciences **25(1)** (2002), 27-31.
[13] M. Kevin, M.B. Rasmus, A.H. Daniel, B.J. Tyler and A.B. Peter, The impact of global signal regression on resting state correlations: Are anticorrelated networks introduced, NeuroImage **44** (2009), 893-905.

[14] M. Hampson, N. Driesen, J.K. Roth, J.C. Gore and R.T. Constable, Functional connectivity between task-positive and task-negative brain areas and its relation to working memory performance, Magnetic Resonance Imaging **28(8)** (2010),1051-1057.
[15] C. Catie and H.G. Gary, Time-frequency dynamics of resting-state brain connectivity measured with fMRI, NeuroImage **50** (2010), 81-98.
[16] D.X. Wu and S.Q. Yao, A novel method for spatio-temporal pattern analysis of brain fMRI data, Science in China, Series *F* **48** (2005), 151-160.
[17] B. György, Rhythms of the Brain, Oxford University Press, 2006.
[18] J.L. Mark, D. Mario, T.L. Joseph, P.M. Vincent and D.P. Micheal, Temporal correlations in low frequency BOLD fluctuations reveal functional networks, NeuroImage **11(5)** (2000), s510.
[19] A.T. Smith, A.L. Williams and K.D. Singh, Negative BOLD in the visual cortex: evidence against blood stealing, Human Brain Mapping **21** (2004), 213-220.
[20] M.E. Raichle, A.M. MacLeod, A.Z. Snyder, W.J. Powers, D.A. Gusnard and G.L. Shulman, A default mode of brain function, Proceedings of the National Academy of Sciences USA **98** (2001), 676-682.